Mechanisms Leading to Stable and Efficient Combustion in Lean Burn Gas Engines

W.Cartellieri, F.G.Chmela, P.E.Kapus and R.M.Tatschl

Combustion Research Department
AVL List GmbH
Kleiststrasse 48, A-8020 Graz
Austria

ABSTRACT

One of the main challenges of lean burn open chamber spark ignited gas engines is to achieve a stable and fast burning at the air/fuel ratios and spark timings necessary for the desired low NO_x emission of 1 g/kWh and below. In pursuit of this challenge a novel combustion system for lean burn gas engines called TRI-FLOW fulfilling these requirements was developed at AVL. In the present paper it is demonstrated how advanced multi-dimensional computational fluid dynamics calculations of mean flow velocity, turbulence, and progress of combustion have been integrated into the development process of the TRI-FLOW combustion system. After giving a general view of the challenges with lean burn gas engines, the evolutionary TRI-FLOW development procedure will be outlined. Flow and combustion patterns as calculated by the FIRE code in a conventional bathtub bowl and in two TRI-FLOW chambers will be presented. Correlating this data with experimentally determined combustion parameters allows to identify the mechanisms leading to stable and fast burn conditions in TRI-FLOW combustion chambers.

INTRODUCTION

In response to the ever tightening exhaust emission standards for NO_x and particulate matter around the world in recent years, natural gas (NG) is now seriously considered as a means of reducing exhaust emissions when used as an alternative fuel in automotive or industrial medium- and heavy-duty diesel engines (buses and commercial vehicles e.g. garbage trucks, power generation and co-generation systems). In converting this category of diesel engines to operation on natural gas particulates are essentially eliminated. To reduce NO_x, HC and CO there are two possible emission control technologies established today, namely (i) open chamber spark ignition of stoichiometric air/fuel mixture with a three-way exhaust catalytic converter for simultaneous NO_x, HC and CO emissions control, and (ii) open chamber spark ignition of lean mixtures for NO_x control in conjunction with an oxidation catalyst for HC and CO emission control. In the past heavy-duty diesel engine conversions into lean burn gas engines were favoured due to their higher thermal efficiency and potential for higher BMEP-level, the latter being comparable to that of turbocharged and intercooled diesel engines, since this boosting technology is equally applicable to lean burn gas engines (References 1 - 10).

One of the main challenges of open chamber lean burn gas engines is to achieve a stable and fast combustion at air/fuel ratios and spark timings necessary for achieving the desired low NO_x-emission. For a satisfactory operating behaviour cycle-by-cycle variations have to be maintained within acceptable limits. A fast heat release is mandatory in order to achieve competitive thermal efficiency while benefiting from the low NO_x emissions achievable under lean burn conditions. As a consequence, a variety of bowl shapes have been conceived and developed at various places in recent years which in principle follow two strategies. The first is relying on low turbulence combustion with its inherent lower NO_x-formation and thus reduced requirement for lean operation (3). The second strategy is aiming at generating a certain in-cylinder flow pattern in conjunction with either intake swirl and/or squish in order to promote flame kernel development at the spark plug and flame propagation throughout the combustion chamber (1, 2, 4 - 10). To achieve low NO_x emission along this "turbulent" route even leaner operation than with the first (low turbulence) strategy is required, due to the higher NO_x-formation associated with faster burning. However, the potential of higher efficiency and better combustion stability along this route is attractive enough to be pursued further.

As a consequence of these considerations a novel lean burn combustion system called TRI-FLOW has been developed at AVL in the last three years along the "turbulent" route. The objective of this programme was to achieve NO_x emission levels as low as with stoichiometric three-way-catalyst systems while approaching diesel like thermal efficiency and BMEP level. Some results of this development programme have already been published elsewhere (11, 12, 13). In the present paper it is to be demonstrated how computational fluid dynamics (CFD) calculations have been integrated into the development process of the TRI-FLOW combustion system. At first, a general view of the challenges with lean burn gas engines will be given. Then, the evolutionary development process of

the TRI-FLOW combustion chamber will be outlined and its performance achievements presented. After a section explaining the calculation methods and the combustion model, flow and combustion patterns in a conventional combustion chamber and in two TRI-FLOW chambers will be presented as calculated by the CFD code FIRE having been developed at the authors' company (14, 15, 16, 17, 18). Correlating this data with experimental results allows to identify the mechanisms leading to stable and fast burn conditions in TRI-FLOW combustion chambers.

CHALLENGES WITH LEAN BURN GAS ENGINES

Fig. 1 shows the typical behaviour of an Otto-Cycle open chamber spark ignited gas engine with regard to exhaust emissions of NO_x, HC and CO when increasing the air excess ratio λ from stoichiometric ($\lambda=1$) to lean ($\lambda>1$) . To achieve NO_x emissions as low as 1 g/kWh under lean conditions, which is the NO_x-level of $\lambda=1$ three-way catalyst (TWC) systems, the air excess ratio needs to be increased at least up to 1.6 (the precise λ is also depending on spark timing and intake manifold temperature and burn rate). As a result, CO and HC increase so that an oxidation catalyst is required in order to reduce them to levels normally seen with $\lambda=1$ TWC-systems. The magnitude of the necessary conversion rates of HC and CO in the oxidation catalyst is indicated by arrows in Fig. 1.

Fig. 2 shows, supplementary to Fig. 1, the remarkable increase of brake thermal efficiency when going lean. This increase of engine efficiency is the result of two countercurrent effects: On the one hand the thermal efficiency increases thermodynamically at the higher air excess ratios, and this effect is enhanced by reduced wall heat losses at the reduced gas temperatures. On the other hand the thermal efficiency is decreasing with increasing λ-ratios as the rate of heat release is continuously slowing down with leaner mixtures. Therefore the full thermal efficiency potential of lean operation can only be used totally when the combustion process is equally fast as it is at stoichiometric operation.

As shown in Fig. 2 there is a significant decrease of exhaust temperature (from about 830°C to 650°C from $\lambda=1$ to $\lambda=1.6$) being conducive in reducing the thermal load of pistons and cylinder heads, but the lower temperature is also increasing the demands on oxidation catalyst conversion efficiency. Also shown in Fig. 2 is the progressive increase of coefficient of IMEP-variations (CIV, that is the standard deviation of IMEP of a certain number of combustion cycles divided by the mean IMEP, expressed in percent) when approaching the lean limit. In the example shown for a conventional combustion chamber, CIV increases to 12% at $\lambda=1.6$ which is necessary for NO_x of 1 g/kWh. However, in practice, CIV of 5% is the upper limit tolerated in power generation and for driveability reasons in automotive applications.Thus, the real challenge in low NO_x lean burn operation is to achieve stable and fast combustion with CIV well below 5%.

EVOLUTIONARY DEVELOPMENT PROCESS

Design Rules of Combustion Chambers

In designing lean burn combustion chambers two hypothetical rules have been kept in mind:

1-To improve combustion stability:
Control of mean flow velocity at the spark position in order to prevent the ionised atmosphere between the spark plug electrodes from being blown away, and to increase turbulent kinetic energy around the spark area for quick flame kernel growth

2-To accelerate combustion progress:
Maximisation of the turbulent kinetic energy level throughout the combustion chamber for enhancement of flame propagation.

These rules have been derived from screening tests of this programme and are in line with research on flame kernel development having been performed at various places in recent years (19, 20, 21, 22). Similar rules have been pursued by others in improving lean burn combustion (1, 6, 7) but so far only in (7) some experimental flow and turbulence data have been successfully correlated with the combustion behaviour of different combustion chambers.

In the present case of the TRI-FLOW chamber development the flow within the chamber was calculated by the CFD code FIRE in order to prove the hypothetical rules stated above and to identify directions for further improvement.

Test Engine

The TRI-FLOW development work was carried out on a turbocharged and intercooled (TCI) 9.6 litre heavy-duty truck engine which was converted from direct injection diesel to open chamber spark ignition.

Main specifications and features of the engine are listed in Table 1. The spark plug is located at the original position of the injector slightly shifted away from the centre of the cylinder. By positioning the gas admission device upstream of the inlet of the turbo-compressor a homogeneous mixture of air and gas was provided to each cylinder. Maintaining turbocharging and intercooling allowed operation at very high BMEP levels competitive with advanced low emission heavy-duty diesel engines.

The use of intake swirl at the same level as with the original diesel engine has been maintained as one of the ingredients mandatory for increased turbulence in lean burn engines.

Development Procedures

All engine testing was performed with natural gas of the properties listed in Table 2. In order to expedite the development process on the engine test bed a new procedure was pursued by taking advantage of development tools available at the authors' company. First of all, each of the 6 cylinders was equipped with a cylinder pressure transducer (AVL type 8QP500ca). Furthermore, in the first phase of

combustion chamber assessment each cylinder was equipped with a different combustion chamber in the piston. Cylinder pressures from each cylinder were simultaneously monitored and recorded on the test bed by an AVL Indiscope type 647. This data acquisition system also provides the function of calculating the coefficient of imep variation (CIV) during a preselectable number of engine cycles. In this case 256 cycles were taken for CIV-assessment. Another function of the data acquisition system provides the calculation of rate of heat release (ROHR) from the mean pressure trace of the 256 cycles. Thus, combustion stability (CIV) and burn rate (ROHR) could be assessed immediately for all six combustion chambers at a time for different loads, speeds, spark timings, and air excess ratios.

Table 1

Specifications and features of TRI-FLOW test engine
- Displacement 9.6 litre - Bore x Stroke 121ø x 140 mm - 6 cylinders, in-line - 2 valves/cylinder - Intake swirl by helical intake ports Swirl level 2.6 (AVL swirl number) - Combustion chamber in piston - Compression ratio 12:1 - Turbocharged, with waste gate - Air/air intercooled - Gas admission system from Deltec positioned before turbo-compressor - Spark ignition by Altronic DIS600 high energy capacitor discharge system

As an example, cylinder pressure traces of six different combustion chambers tested simultaneously at high load (BMEP 9.6 bar) and λ=1.61 are shown in Fig. 3, and at low load (BMEP 2 bar) and λ=1.50 in Fig. 4. In Figs. 3 and 4, also appertaining CIV values are shown on the pressure traces. CIV-ratings were then also plotted versus the air excess ratio λ, as shown typically for six chambers in Fig. 5.

Table 2

Properties of natural gas (by Vol.%)	
CH_4	98%
C_2H_6	0.7%
C_3H_8	0.2%
C_4 +	0.1%
CO_2	0.2%
N_2	0.8%
Lower heating value	48.635 MJ/kg
Methane No.	92

Along this procedure a variety of combustion chambers having been designed in pursuit of special strategies (e.g. squish flow, diverted intake swirl, or a combination of both) was evaluated for CIV and ROHR. As these chambers were designed to determine the strength of a certain parameter, e.g. to evaluate increasing squish by increasing squish area, an evolutionary development of the combustion behaviour was possible. As a consequence of each test run, the best chambers were selected and modified for the next step for further improvement.

This experimental process was supported in parallel by multi-dimensional calculations of flow velocity and turbulence patterns (by FIRE) of promising combustion chamber shapes (as identified by the experimental procedure mentioned before), in order to better understand the in-cylinder processes and to derive guidelines for further improvements. As a result of this procedure certain criteria for a stable and fast combustion process were identified and finally verified in the TRI-FLOW design, as described in more detail in a later section.

Performance achievements of the TRI-FLOW combustion system

As a result of this development process a low NO_x lean burn combustion system with very attractive performance was established. Full load and part load achievements of the 9.6 litre TCI NG-engine with TRI-FLOW combustion system are shown in Figs. 6 and 7, respectively. It has to be noted that under all of these test conditions NO_x was maintained at 1 g/kWh, and the coefficient of IMEP-variation was around 2% or below. Furthermore it is shown that full load BMEP and brake thermal efficiencies are competitive with those of highly turbocharged heavy-duty DI diesel truck engines. Part load efficiency above BMEP of 6 bar was improved by avoiding throttling losses by means of a specially designed waste gate which allows to control part load operation at fully open throttle. Thus the throttle is operated only below BMEP of 6 bar, above 6 bar BMEP the engine is operated unthrottled, and the load is controlled by the waste gate only.

FLOW AND COMBUSTION MODELLING

Calculation Method, Mathematical Framework

The computational fluid dynamics code system FIRE solves the density-weighted ensemble-averaged differential conservation equations of mass, momentum, and stagnation enthalpy in addition to the transport equations of the k-ε turbulence model in three space dimensions and time. In the case of reactive flows, additional conservation equations are solved in order to determine the thermochemical state of the mixture and the mean rate of chemical heat release.

The hydrocarbon oxidation process is expressed, following the common practice, by a single-step irreversible combustion reaction of the form

$$1\,[kg]\,\text{Fuel} + \frac{S}{0.232}[kg]\,(0.232O_2 + 0.768N_2) \rightarrow (1+S)[kg]\,\text{Products} + 3.31\,S\;[kg]\,N_2 \qquad \text{Equ. (1)}$$

where S is the stoichiometric oxygen requirement per unit mass of fuel.

Combustion Model

In order to express the reactive system, partial differential transport equations for the mixture fraction "f" and the probability density function (PDF) of a reaction progress variable "c" are solved (23). The numerical integration of these conservation equations enables the determination of the mean rate of chemical reaction fully taking into account the turbulence/chemistry interaction and thus obviating the need for any prior assumptions as to whether one or the other process is controlling the mean rate of combustion. With the aid of auxiliary relations the determination of composition fields and the thermochemical state of the charge is enabled. The conservative scalar variable f is equivalent to the total (burnt + unburnt) fuel mass-fraction and thus a measure of the mixing between the air and the fuel, irrespective of their taking part in the combustion process. Therefore, in the present case of homogeneous premixed charge combustion f is a constant value, independent of space and time. The reaction progress variable c is equivalent to the reaction product mass-fraction normalised by the maximum product mass-fraction that can occur such that either all the fuel or all the oxidant is depleted. It is evident that c is bounded by the values of zero and unity corresponding to the unburnt and burnt states, respectively, regardless of the equivalence ratio.

Adopting the standard gradient diffusion approximation and a stochastic mixing model (24) for modelling turbulent convection in physical space and molecular mixing in composition space, the modelled transport equation for the reaction progress variable probability density function $p_{(c)}$ can be written in the form

$$\frac{\partial}{\partial t}\left\{\overline{\rho}\,\tilde{p}_{(c)}\right\}+\frac{\partial}{\partial x_j}\left\{\overline{\rho}\,\tilde{U}_j\tilde{p}_{(c)}-\Gamma_c\frac{\partial\tilde{p}_{(c)}}{\partial x_j}\right\}=$$

$$\frac{\partial}{\partial c}\left\{\overline{\rho}\,\tilde{p}_{(c)}s_{(c)}\right\}+\overline{\rho}\,\frac{2C_{mi}}{\tau}\left\{\int_0^c\tilde{p}_{(c-c')}\tilde{p}_{(c+c')}dc'-\tilde{p}_{(c)}\right\}$$

Equ .(2)

where $p_{(c)}$ is the probability that at location x and time t the quantity c is within the range $c < c < c+dc$. The mean density is then given by

$$\overline{\rho}=\left\{\int_0^c\frac{\tilde{p}_{(c)}}{\rho_{(c)}}dc\right\}^{-1}\qquad\text{Equ. (3)}$$

In the above, ρ is the mixture density, U_j are the components of the velocity vector and Γ_c is the diffusion coefficient. In the present case of turbulent flow, the diffusion coefficient is calculated based upon the solution of the k-ε equations.

In equation (2) $\tau = k/\varepsilon$ is the turbulent mixing time and C_m a model constant. The first term on the right hand side of equation (2) represents the effect of chemical reaction, and $s_{(c)}$ is assumed here to be of the standard Arrhenius type.

Solution Method

The partial differential transport equations governing general compressible reacting flows are recast into the curvilinear non-orthogonal form and transformed to an Eulerian-Lagrangian coordinate system, so to enable their solution on body-fitted computational grids with moving boundaries. The differential transport/conservation equations governing mean fluid motion are discretised adopting the finite-volume approach. The temporal integration is Euler implicit, in order to ensure unconditional numerical stability, and for approximation of the spatial derivatives a hybrid central/upwind differencing scheme is used. This practice leads to coupled algebraic equation systems solved iteratively on a SIMPLE based pressure-velocity coupling procedure. The PDF transport equation for the reaction progress variable c is solved using a Monte Carlo simulation approach in which the continuous probability density function $p_{(c)}$ is represented by an ensemble of notional elements located at the cell centres of the finite-volume computational mesh (25). In order to advance the PDF from time t to $t+\Delta t$ the notional elements are transported across physical and composition space according to the processes of convection, diffusion, reaction, and mixing, simulated sequentially based upon an explicit operator splitting method.

The solution of the coupled equation systems of the hybrid finite-volume mean flow/Monte Carlo PDF method is advanced from the initial conditions in a time marching method, updating velocity, pressure, and mean scalar fields according to the solution of the Monte Carlo simulation that determines the thermochemistry of the mixture.

Calculation Procedure

The calculations commenced at inlet valve closure (140 deg. crank angle before firing top dead centre) with a prescribed swirling velocity field according to values obtained on a steady flow test rig adopting the paddle-wheel method. The thermodynamic initial conditions were taken according to the measured inlet manifold data.

The ignition process is simulated through prescription of the temporal variation of the reaction progress variable c in a number of computational cells at the spark location. An 's'-shaped variation over a 4 degree crank angle period has been used in the present calculations. Although the mean value of the reaction progress variable is thus fixed, there exists an infinite number of possible PDF shapes that satisfy this. "Maximum" variance ignition has been used in the present case.

ENGINE TEST AND FIRE CALCULATION RESULTS

Combustion Chamber Geometries

Within the scope of this paper the presentation of results will be limited to three combustion chamber shapes. Fig. 8 shows in axonometric form the computational meshes

of the three chambers in their position of 20 degree crank angle before top dead centre (BTDC). All three bowls are located in the piston crown, and the cylinderhead firedeck plane is forming the upper boundary surface of the chamber geometry. All three bowls are operated with intake swirl (swirl number 2.6) which is rotating clockwise when looking from top onto the chambers in Fig. 8.

The conventional axisymmetric bathtub chamber being positioned off-center towards the exhaust valve (for directed squish into a hot zone) is selected for reference in order to demonstrate deficiencies leading to slower and less stable burning under lean conditions. The TRI-FLOW I chamber represents an intermediate status of the development process, whereas the TRI-FLOW II chamber is one of the latest design versions. Both are located centrically below the spark position.

Combustion Stability and Rate of Heat Release

Figs. 9 and 10 show combustion stability in terms of CIV as a function of the air excess ratio λ at 2000 rpm/BMEP 10 bar and 1500 rpm/BMEP 10 bar, respectively. Under both operating conditions, it is obvious that all three bowls are about equally stable (well below CIV 2.5%) as long as λ stays below about 1.45. Above this λ-value, however, CIV of the conventional bowl increases dramatically whereas the TRI-FLOW II chamber is approaching the critical CIV limit of 5% not until λ=1.7 (1500 rpm) to λ=1.8 (2000 rpm). At CIV of 5%, the TRI-FLOW I chamber is about 0.05 to 0.10 λ-units less tolerant than the TRI-FLOW II chamber.

Fig. 11 shows rate of heat release and accumulated heat release at constant air excess ratio λ=1.6 (2000 rpm/10 bar BMEP). Spark timing was set at 20° crank BTDC. It is obvious that the rate of heat release is increased in all combustion phases (initial phase and main phase) when changing from the conventional chamber to the TRI-FLOW I and II chamber, respectively. The favourable behaviour of the TRI-FLOW bowl shapes is obviously the result of special flow effects affecting both CIV and ROHR, as shown in the following sections.

Mean Flow Velocity and Turbulence

Mean flow velocity and turbulence distributions within the combustion chambers were calculated by the FIRE code at the following operating conditions:

- Engine speed 2000 rpm
- BMEP 10 bar
- Spark timing 20° crank BTDC
- Air excess ratio (λ) 1.6

These conditions correspond to the ROHR-cases shown in Fig. 11, and the appertaining CIV-values are indicated in Fig. 9.

Mean flow velocity fields in three sections through the three combustion chambers at the crank angle of spark timing (20° BTDC) are shown in Fig. 12(a-c). In this Figure the sections through the bowls' geometry within the computational mesh are indicated in red. Since the flow conditions around spark location have been found to be most important for flame kernel development (19, 20, 21, 22) attention will be drawn to this fact in the following considerations.

In Fig. 12a for the conventional bowl it can be seen that at the spark location there is a strong cross flow due to overshooting swirling squish from the clearance volume, whereas in the TRI-FLOW chambers, Figs. 12b and 12c, there are much lower mean velocities, and a stagnation area near the spark plug is being formed as a result of the combination of squish and diverted and colliding swirl motion being generated by the combustion chamber shape.

Histories of mean flow velocity and turbulent kinetic energy (TKE, defined as (3/2 $\overline{u'^2}$) where u' is the isotropic turbulent velocity) at the location of the spark under non-firing conditions are shown in Fig. 13. There are several peculiarities in both, mean velocity and TKE. The cross flow already seen with the conventional chamber in Fig. 12a, is increasing further after spark timing and reaches a maximum near TDC, whereas the mean flow velocities of the TRI-FLOW II chamber remain at the low level. The TRI-FLOW I chamber exhibits a behaviour in-between the other two chambers. As far as turbulence at the spark location is concerned Fig. 13 shows clearly a steep increase of TKE towards TDC for the TRI-FLOW II chamber whereas the TKE levels of the conventional chamber, but also the TRI-FLOW I chamber are much lower and not significantly different from each other. However, the history of the cylinder-mean TKE integrated over the whole combustion space (i.e. over the chamber volume plus the disc shaped piston to top clearance volume), as shown in Fig. 14, exhibits a gradual increase in turbulence level when changing from the bathtub to TRI-FLOW I and further to TRI-FLOW II.

Correlation of Combustion and Flow Parameters

It is appropriate now, to correlate experimentally determined CIV and ROHR data with calculated mean velocity and TKE data. In doing so, Fig. 15 shows correlations for:

- Mean flow velocity at spark location at 10° crank BTDC vs. CIV (Fig. 15a) and vs. degree crank duration for 10% mass burnt (Fig. 15b)
- TKE at spark location at 20° and 10° crank BTDC vs. degree crank duration for 10% mass burnt (Fig. 15c)
- Peak cylinder-mean TKE vs. peak ROHR (Fig. 15d)
- Peak cylinder-mean TKE vs. degree crank duration for 10-90% mass burnt (Fig. 15e).

The correlations in Fig. 15(a-c) are related to phenomena of the initial combustion phase, whereas the correlations in Fig. 15(d-e) are related to the main combustion period.

As to the initial combustion phase it appears, as if CIV was primarily affected by the mean flow velocity at the spark location so that beyond a certain mean flow velocity level CIV increases dramatically. The initial flame growth itself, as characterised by the crank degree interval required to consume 10% of the mass, seems to be affected by both, mean flow velocity (the smaller, the better) and TKE (the higher, the better) at spark location.

The correlations of Fig. 15(d-e) for the main combustion period clearly reflect the well known strong effect of TKE on ROHR and combustion duration.

Multi-Dimensional Progress of Combustion

As part of the development process of the TRI-FLOW combustion chambers, and supplementary to the flow calculations presented in the previous section, also the combustion process was modelled in order to better comprehend the complex interaction of flow velocities and turbulence patterns and their effect on flame development within the various combustion chambers. As a result of these calculations, progress of combustion in the three chambers, under the same conditions as the flow calculations were based on, is shown in Fig. 16(a-c). For each chamber, combustion progress is imaged at four crank angle positions. In each case the flame progress is shown on three planes through the chamber, namely on a horizontal plane located halfway in the disc shaped top clearance volume, and on two planes being perpendicular to the horizontal one and to each other. In the pictures the blue colour represents unburnt mixture, and the red colour completely burnt mixture. The yellow zones indicate the momentary position of the flame front. On each picture the percentile of burnt mass is indicated as calculated by the FIRE code.

Combustion progress in the conventional bowl, Fig. 16a, shows first of all a strong displacement of the flame kernel away from the spark location deep into the ground of the bathtub, as a result of the massive squish velocities from the asymmetric squish area opposite of the bowl. On the one hand, the strong convective flow in the spark area is known to be conducive in activating or igniting larger mixture parcels, on the other hand the ignition energy brought in per unit mass is reduced making the flame kernel prone to being quenched. The latter and the unfavourable asymmetric position of the flame kernel after the ignition phase is obviously dominating and leads to a long ignition delay phase and later on to slowed down flame propagation from the bowl ground towards the cylinder head. At 15 degree crank ATDC only 42.4% of mass is burnt (45% were measured).

Combustion in the TRI-FLOW I chamber, Fig. 16b, is spreading from a flame kernel which is stabilised around the spark plug due to the symmetric squish areas of this chamber design causing a stagnating flow area around the spark. Combustion then progresses symmetrically from the spark position into the chamber, but due to the off-center position of spark and chamber there is finally a slightly asymmetric flame front. At 15 degree crank ATDC 77.5% of mass is burnt (65% were measured).

Combustion progress in the TRI-FLOW II chamber, Fig. 16c, is characterised by fast growth rate of the flame kernel which again is stabilised and centralised in its position near the spark by the symmetric flow towards this area, and which is also due to very low mean flow velocities but very high turbulence level in the centre and throughout the whole chamber. As a result, the flame propagates quickly and rather symmetrically into the individual parts of the chamber, so that at 15 degree crank ATDC 77.0% of the mass are burnt (80% were measured). This fast burning is also reflected in Fig. 16c by the dominion of the red colour filling nearly completely the whole chamber at 15 degree crank ATDC.

SUMMARY AND CONCLUSIONS

In recent years spark ignited lean burn open chamber natural gas engines having been converted from heavy-duty diesel engines have become increasingly attractive in automotive and industrial applications due to their potential for low NO_x and particulate exhaust emissions, high thermal efficiency, and high BMEP level.

One of the main challenges of this engine category is to achieve stable combustion at the lean air/fuel ratios necessary for lowest NO_x emissions. In taking up this challenge an open chamber lean burn combustion system called TRI-FLOW has been established at AVL which allows to achieve NO_x emissions as low as 1 g/kWh while maintaining stable combustion (coefficient of IMEP variation CIV $\leq$ 2%) and diesel-like efficiency at diesel-like BMEP-levels.

In elaborating the TRI-FLOW system novel experimental techniques and computational fluid dynamics (CFD) calculations have been integrated into the development process in order to expedite the evolution of the combustion chamber shape. CFD calculations by the FIRE code for mean flow velocity, turbulence, and combustion progress within the chamber were performed in parallel to the experimental development process on the testbed using a turbocharged and air/air intercooled 9.6 litre in-line 6-cylinder engine (operated on natural gas), which had been converted from a heavy-duty truck diesel engine. Thus, flow data could be correlated with combustion parameters in order to identify mechanisms for stable and fast combustion.

As a result of these investigations which are exemplified in this paper on a conventional bathtub bowl and on two combustion chamber versions of the new TRI-FLOW system, the following conclusions with regard to the mechanisms for stable and efficient combustion can be drawn:

- Combustion stability in terms of CIV under lean conditions ($\lambda \geq 1.5$) appears to be affected primarily by the mean flow velocity at the spark location at the time of and after spark. Beyond a certain mean flow velocity level CIV increases dramatically.

- Initial flame growth seems to be affected by both, mean flow velocity (the smaller, the better) and turbulent kinetic energy (TKE; the higher, the better) at spark location.

- Rate of heat release (ROHR) of the main combustion period is mainly affected by the level of cylinder-mean turbulent kinetic energy. The higher the latter, the higher peak-ROHR and the shorter combustion duration.

- Multi-dimensional modelling of progress of combustion in the various chambers revealed that in the TRI-FLOW

chamber there is a fast flame kernel growth due to low mean flow velocity but high TKE at spark location. Thus the flame kernel remains stabilised in the centre area of the symmetric chamber. Due to the rather high TKE level in the bulk of the TRI-FLOW chamber the flame propagates quickly and rather symmetrically into the individual parts of the chamber, causing a stable and diesel-like ROHR.

Thus, the integration of CFD calculations by means of the FIRE code into the experimental development process proved to be very efficient in directing the evolution of the TRI-FLOW combustion system.

ACKNOWLEDGEMENT

The authors gratefully acknowledge the contributions of their colleagues in the various departments. Thanks are also due to Mr. Viktor Schedlbauer for all of the graphical work, and to Ms. Christine Schuster for typing the manuscript.

REFERENCES

1. Kingston Jones, M.G., Heaton, D.M, "Nebula Combustion System for Lean Burn Spark Ignited Gas Engines", SAE-Paper 890211, 1989.

2. Duggal, V. "The Natural Gas L10 Urban Bus Engine - an Alternative Fuel Option", Paper C437/062, IMechE, 1992.

3. Cole, J.J., Meyer, R.C., Kienzle, E., Wells, A.D., "Development of the Hercules GTA3.7L and GTA5.6L Engines for Low Emissions using on Open Chamber Lean Burn Combustion System", NGV Conference, Göteborg, 1992.

4. Hammarberg, G., "SCANIA Natural Gas Engine Development", NGV Conference, Göteborg, 1992.

5. Jönsson, L., Larsson, H., "VOLVO THG103 - a Low Emission CNG Engine", NGV Conference, Göteborg, 1992.

6. Mendis, K.J.S., Stone, C.R., Ladommatos, N., "Modelling and Measurements from a Natural Gas Fuelled Engine", SAE-Paper 930927, 1993.

7. Sakurai, T., Iko, M., Okamoto, K., Shoji, F., "Basic Research on Combustion Chambers for Lean Burn Gas Engines", SAE-Paper 932710, 1993.

8. Sharp, C.A., Ullman, T.L., Stamper, K.R., "Transient Emissions from Two Natural Gas-Fueled Heavy-Duty Engines", SAE-Paper 932819, 1993.

9. Athenstaedt, G., "Entwicklung stationärer Gasmotoren seit dem Inkraftreten der TA-Luft (The Effect of TA-Luft on Development Trends for Gas Engines)", MTZ 54 (1993), pp. 602-606.

10. Clarke, D.P., Penny, I.J., Wise, D.A., Das, P.K., "Understanding the Potential of the Non-Aftercooled Navistar 7.3 T CNG Engine", SAE-Paper 940549, 1994.

11. Chmela, F., Kapus, P., "The new AVL High-Turbulence Lean-Burn Natural Gas Engine", IMechE Seminar: Gas Engines for Co-Generation, London, 1993.

12. Kapus, P., Chmela, F., "The new AVL Gas Engine Combustion System", ICE-Vol. 20, Alternate Fuels, Engine Performance and Emissions, ASME, 1993.

13. Chmela, F.G., Kapus, P.E., "The TRI-FLOW Combustion System and its Effects on Lean Burn Gas Engine Performance", Second Enserv European Stationary Gas Engine and Heavy-Duty Utility Vehicle Gas Engine Symposium Workshop, Celle/Germany, 1994.

14. Bachler, G., Brandstätter, W., Steffan, H., Wieser, K., "Dreidimensionale Simulation von Strömungs-, Gemischbildungs- und Verbrennungsvorgängen (Three-Dimensional Simulation of Flow, Mixture Formation and Combustion)", Conference "Der Arbeitsprozeß des Verbrennungsmotors", University of Technology, Graz/Austria, 1989.

15. Tatschl, R., Brandstätter, W., "Multidimensional Calculation of Spark Flame Initiation by Adopting a Generic Hydrocarbon Kinetic Scheme", Computational Methods in Applied Sciences, Elsevier Science Publishers, 1992.

16. Tatschl, R., Brandstätter, W., "The Application of a Hybrid Finite-Volume / Monte Carlo PDF Method to Engine Combustion Simulation", Nato Advanced Study Institute on Unsteady Combustion, Instituto Superior Técnico, Lisboa/Portugal, 1993.

17. Tatschl, R., Wieser, K., Reitbauer, R., "Three-Dimensional Simulation of Inhomogeneous-Charge Combustion in a 4-Valve SI Engine", Second World Conference in Applied Computational Fluid Dynamics, Basel, 1994.

18. Tatschl, R., Wieser, K., Reitbauer, R., "Multidimensional Simulation of Flow Evolution, Mixture Preparation and Combustion in a 4-Valve SI Engine", COMODIA 94, Yokohama, 1994.

19. Keck, J.C., Heywood, J.B., Noske, G., "Early Flame Development and Burning Rates in Spark Ignition Engines and their Cyclic Variability", SAE-Paper 870164, 1987.

20. Pischinger, S., Heywood, J.B., "How Heat Losses to the Spark Plug Electrodes Affect Flame Kernel Development in an SI-Engine", SAE-Paper 900021, 1990.

21. Bloss, W., Herweg, R., Ziegler, G., "Untersuchung der Flammenkernbildung im Ottomotor (Investigation of Flame Kernel Development in Otto-Cycle Engine)", MTZ 51 (1990), pp. 202-209.

22. Bloss, W., Wodarz, J., Köhler, J., "Einfluß realer Motorbedingungen auf die Flammenkernbildung (Effect of Real Engine Conditions on Flame Kernel Development)", MTZ 54 (1993), pp. 300-308.

23. Pope, S.B., "PDF Methods for Turbulent Reactive Flows", Prog. Energy Combust. Sci., Vol. 11, pp.119-192, 1985.

24. Curl, R.L., "Dispersed Phase Mixing: 1. Theory and Effects in Simple Reactors", AICHE Journal, 9, pp. 175-181, 1963.

25. Pope, S.B., "A Monte Carlo Method for the PDF Equations of Turbulent Flow", MIT-EL 80-012.

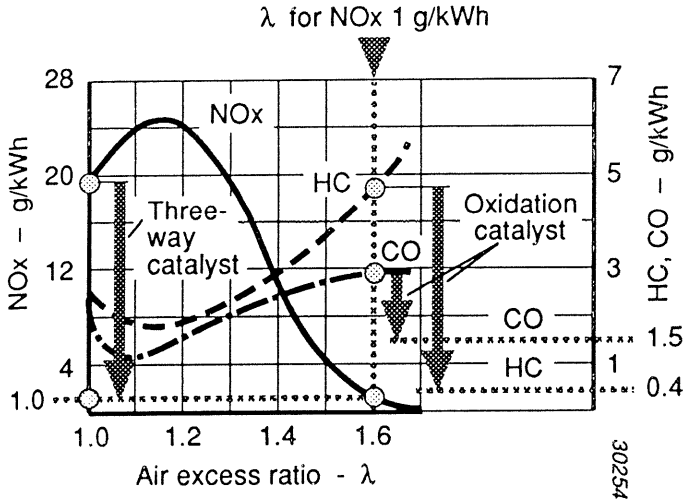

Fig. 1 Effect of air excess ratio on engine-out emissions of open chamber spark ignition gas engine

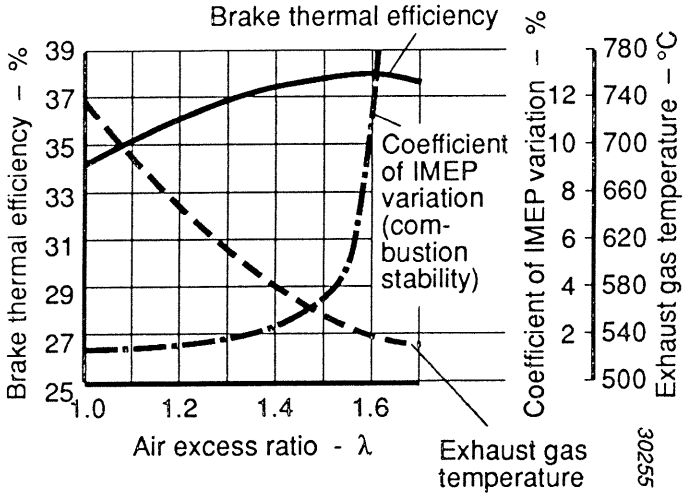

Fig. 2 Effect of air excess ratio on brake thermal efficiency, exhaust temperature and combustion stability

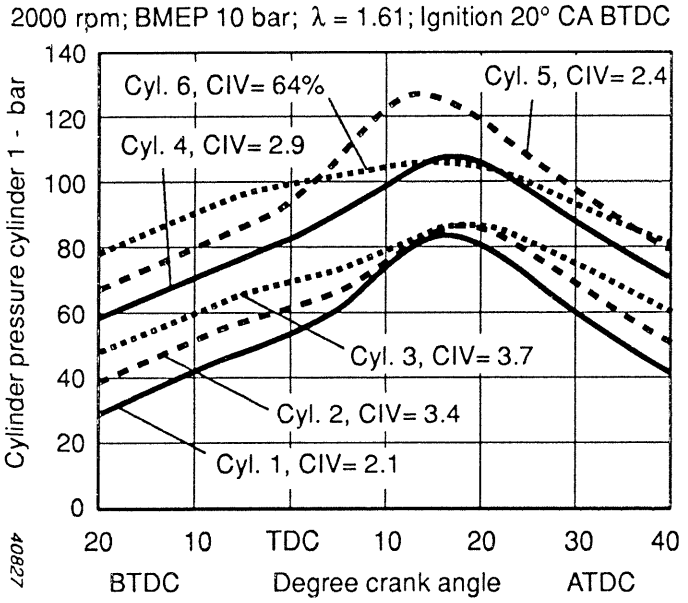

Fig. 3 Cylinder pressure traces of six combustion chambers at high load

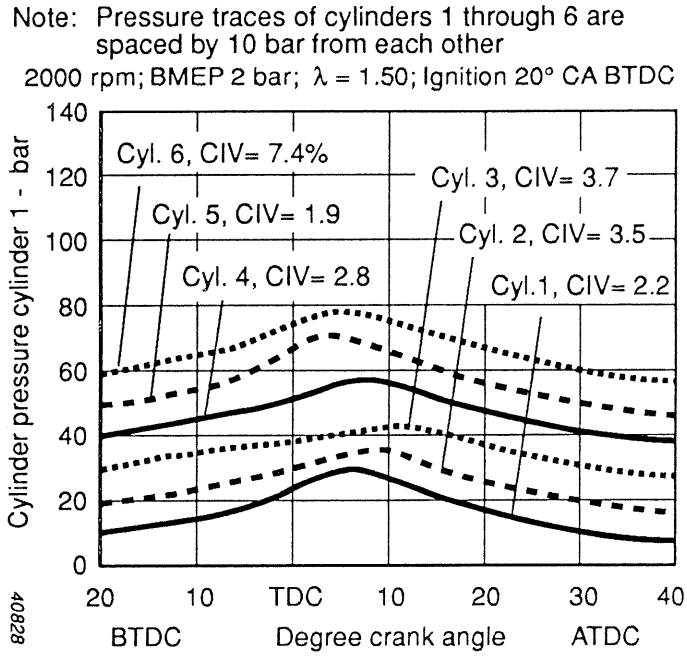

Fig. 4 Cylinder pressure traces of six combustion chambers at low load

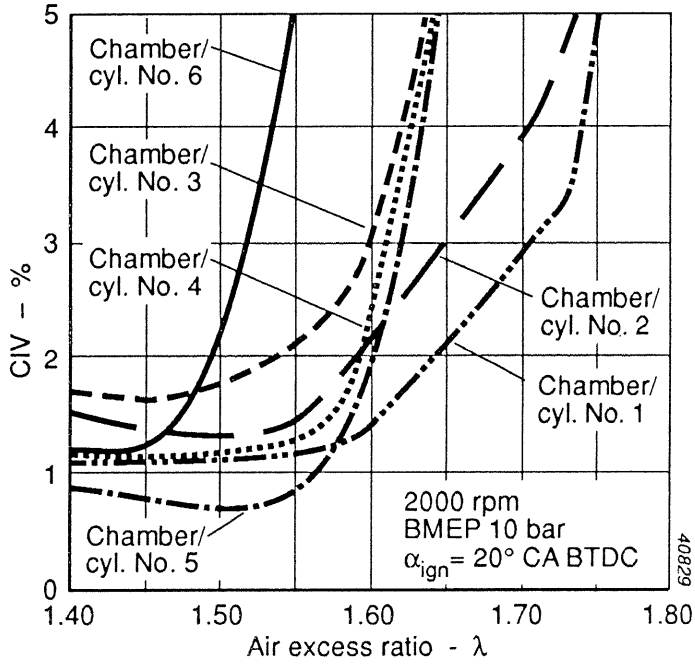

Fig. 5 Coefficient of IMEP variations (CIV) of six combustion chambers

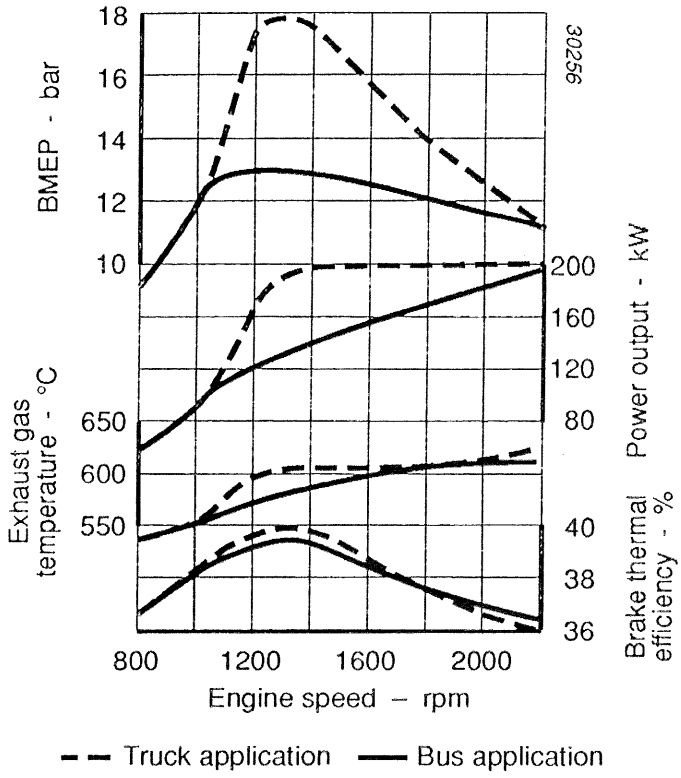

Fig. 6 Full load performance of TRI-FLOW lean-burn NG engine. NO_x 1 g/kWh constant.

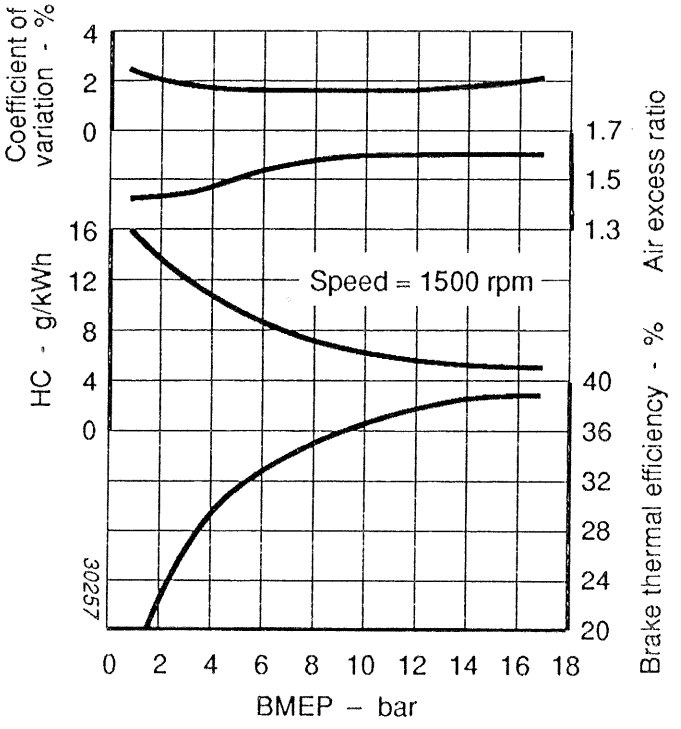

Fig. 7 Part load performance of TRI-FLOW lean-burn NG engine. NO_x 1 g/kWh constant.

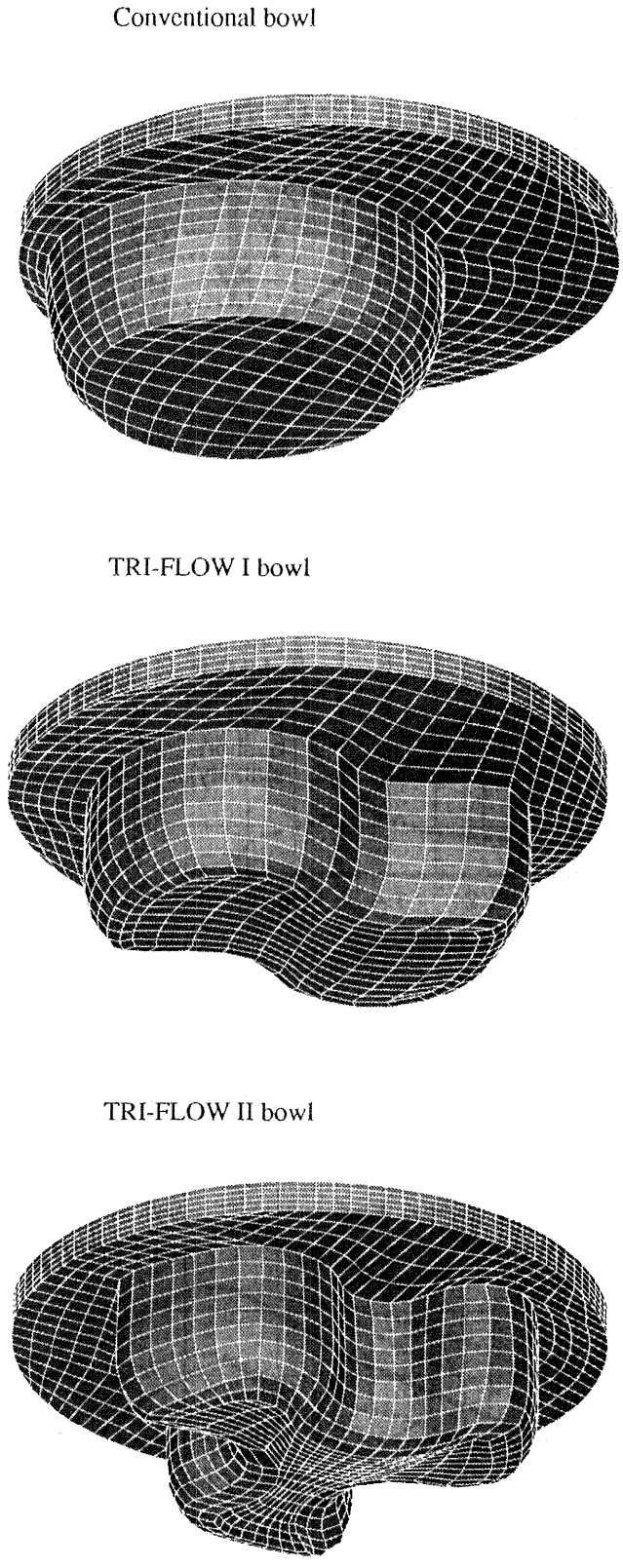

Fig. 8 Combustion chamber geometries

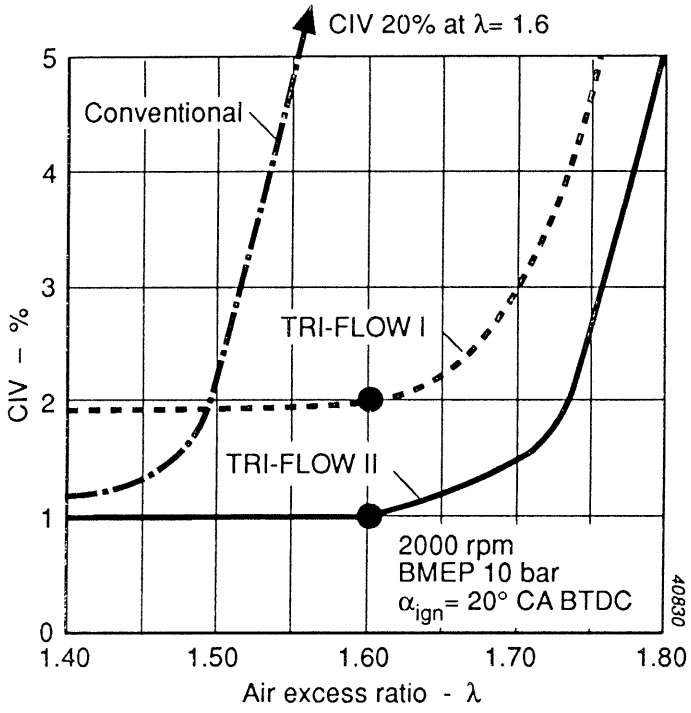

Fig. 9 Coefficient of IMEP variation (CIV) of conventional, TRI-FLOW I and TRI-FLOW II chamber at 2000 rpm / 10 bar

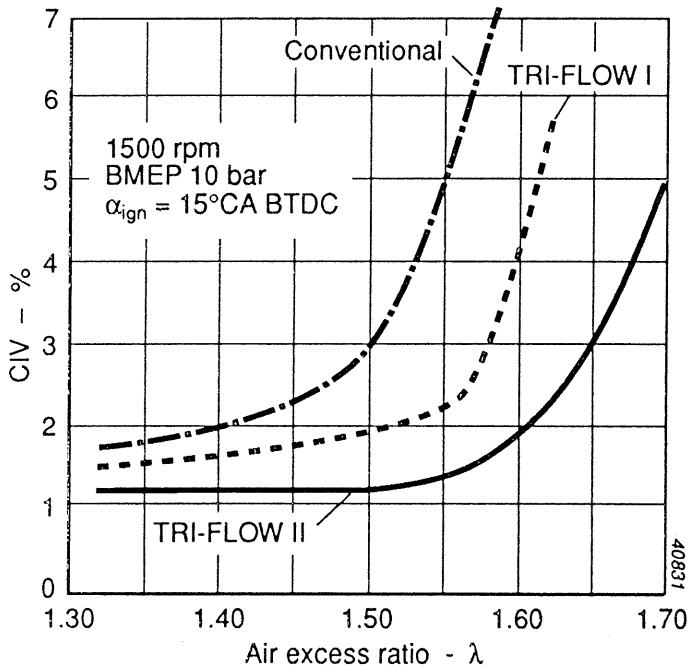

Fig. 10 Coefficient of IMEP variation (CIV) of conventional, TRI-FLOW I and TRI-FLOW II chamber at 1500 rpm / 10 bar

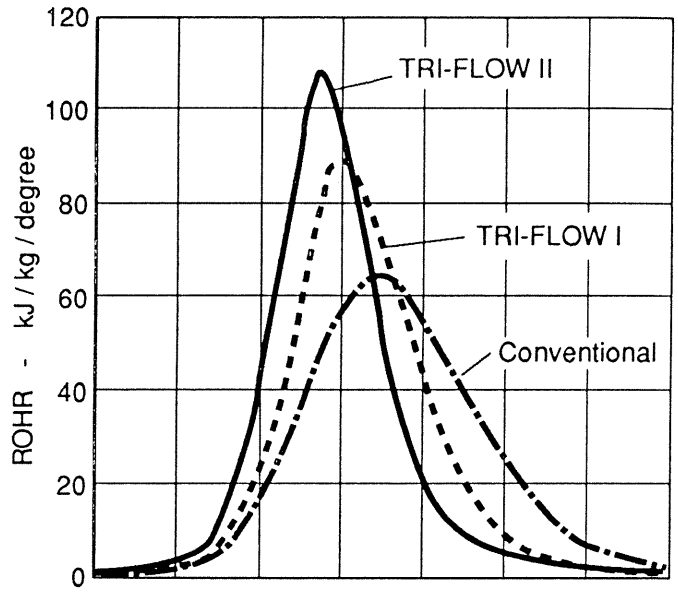

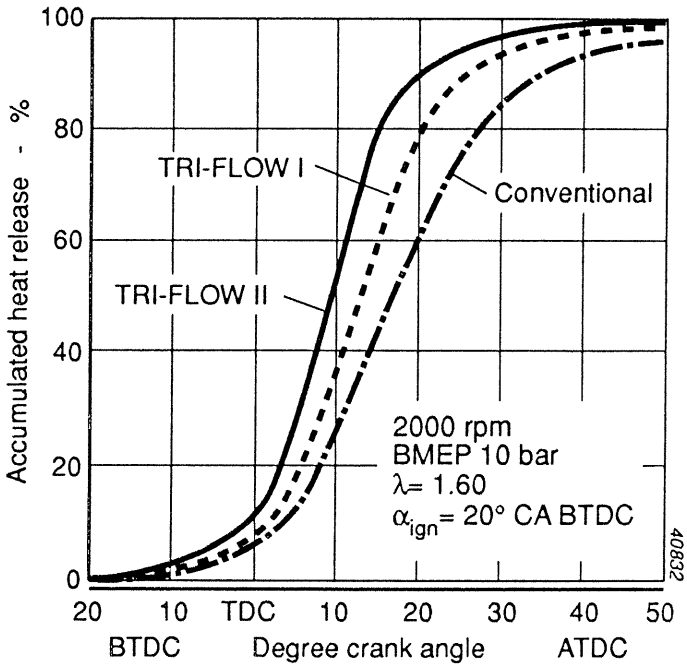

Fig. 11 Rate of heat release (ROHR) and accumulated heat release of conventional, TRI-FLOW I and TRI-FLOW II chamber at 2000 rpm / 10 bar

a) Conventional chamber

b) TRI-FLOW I chamber

c) TRI-FLOW II chamber

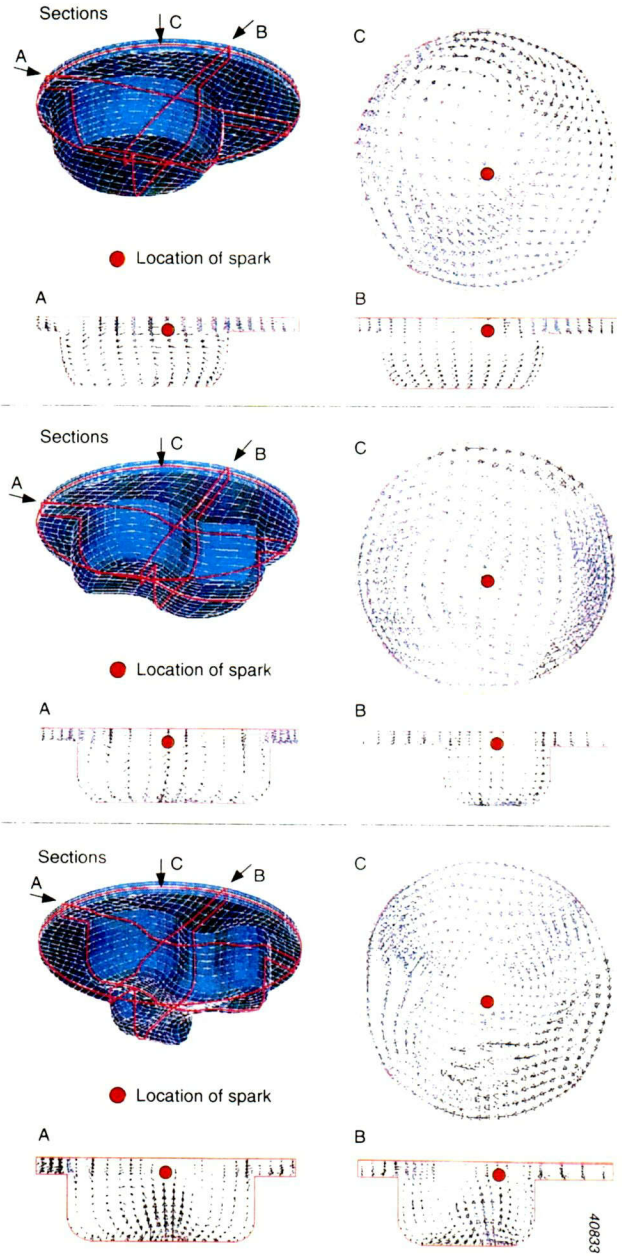

Fig. 12 Flow pattern at spark timing (20 °CA BTDC) in different combustion chambers

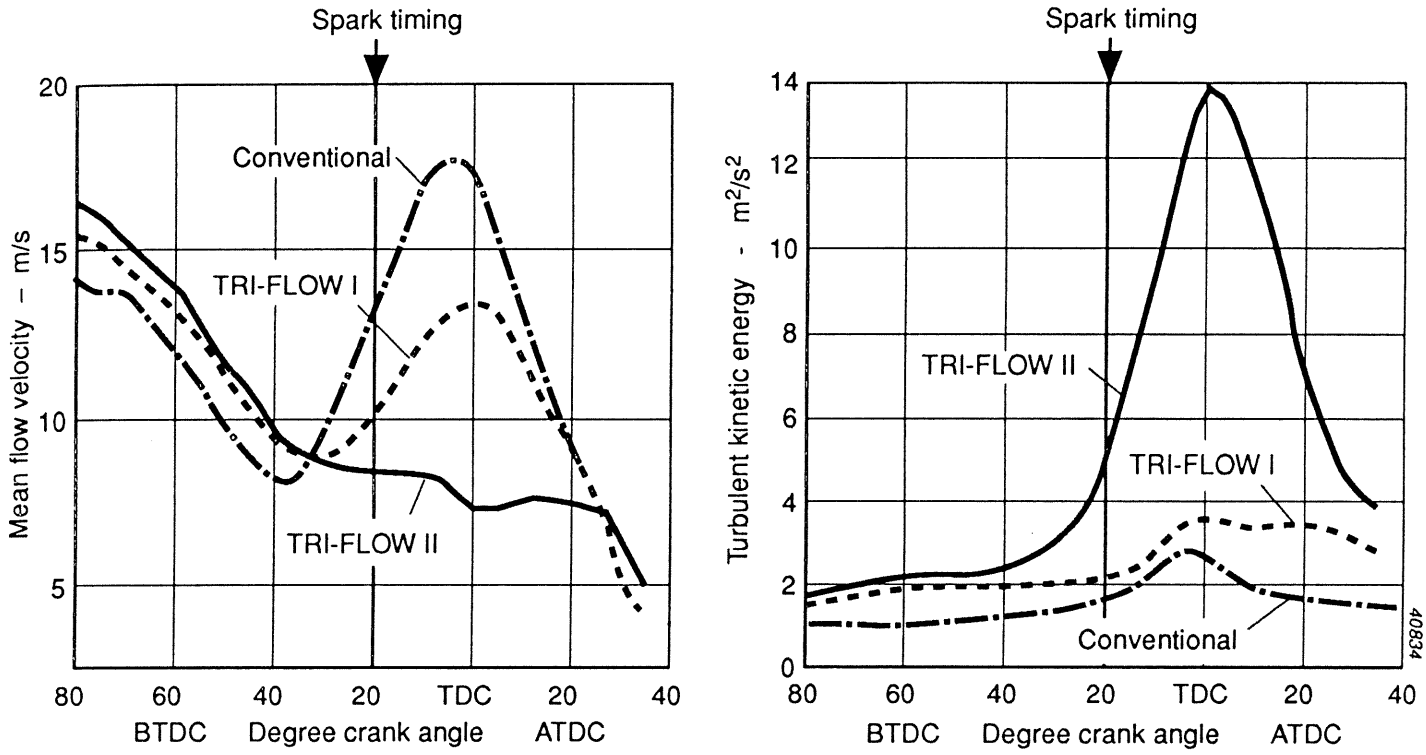

Fig. 13 Mean flow velocity and turbulent kinetic energy at spark location

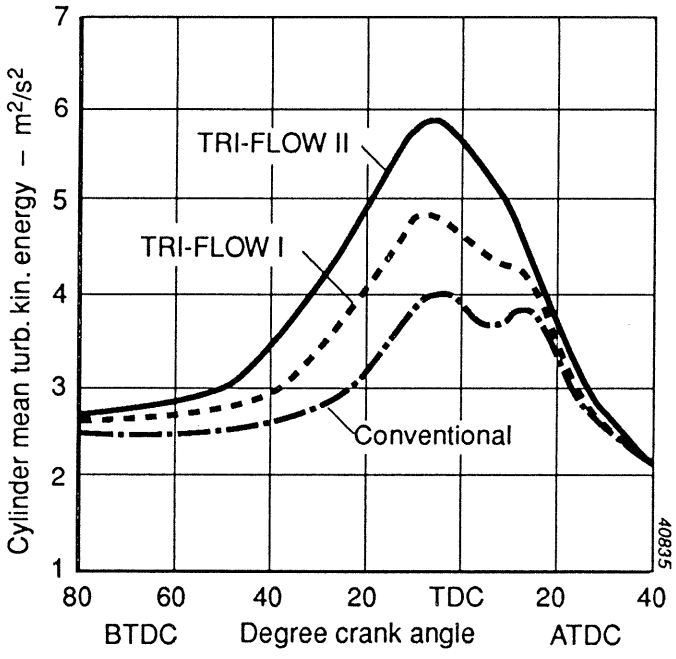

Fig. 14 Cylinder-mean turbulent kinetic energy

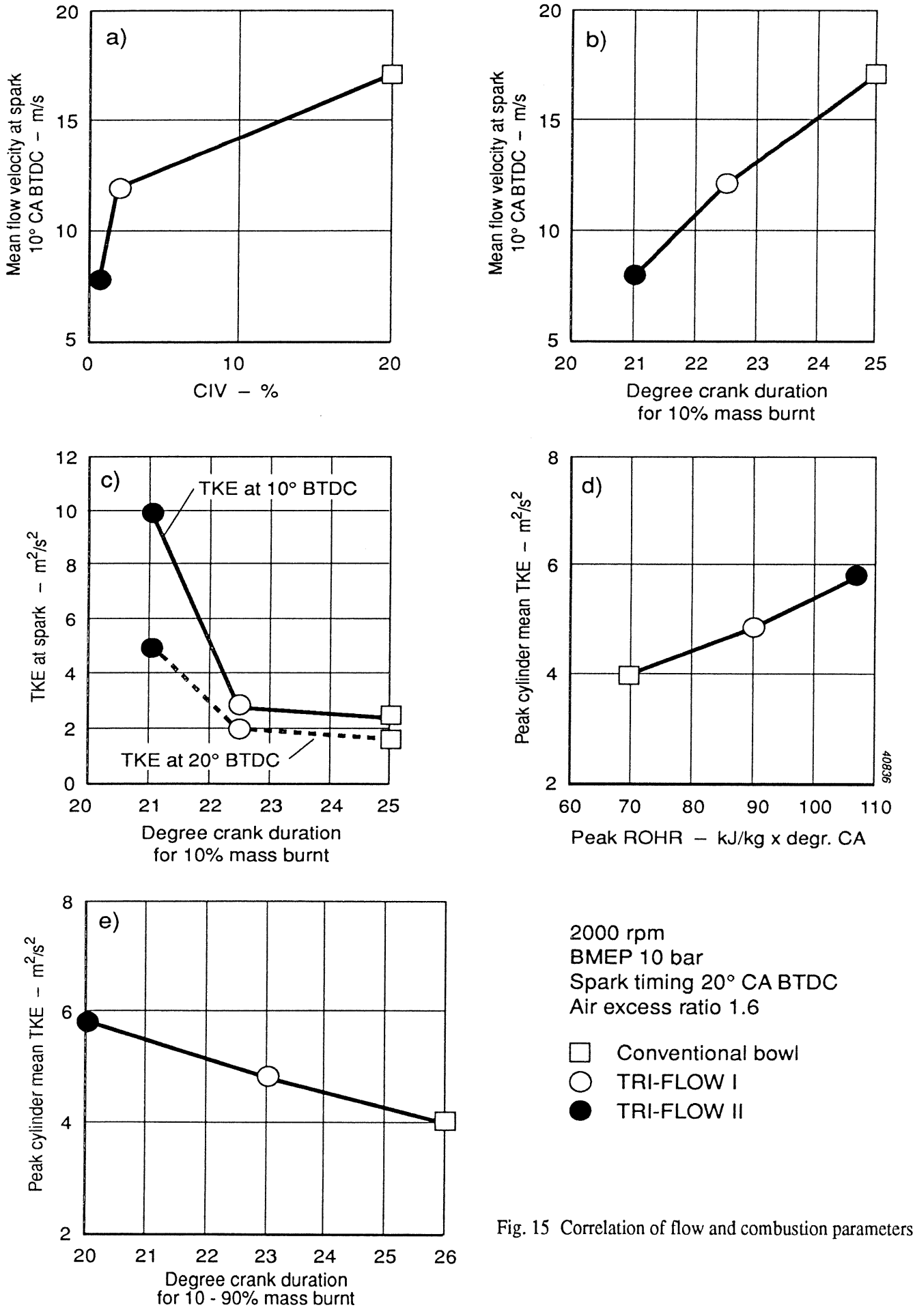

Fig. 15 Correlation of flow and combustion parameters

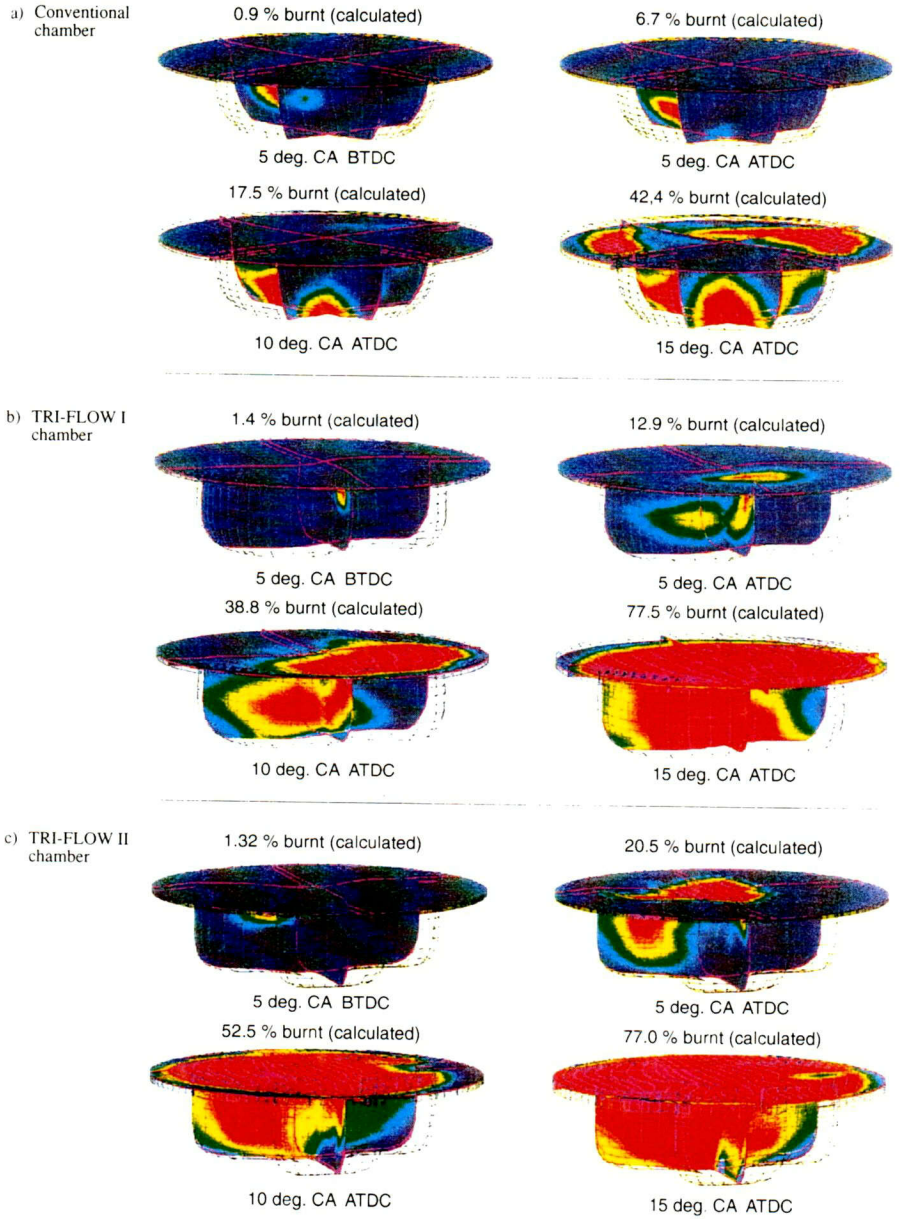

Fig. 16 Progress of combustion in different combustion chambers